Pure & Appl. Chem., Vol. 56, No. 3, pp. 369-384, 1984.
Printed in Great Britain.

0033-4545/84 $3.00+0.00
Pergamon Press Ltd.

POLYMER MELT RHEOLOGY - A CHALLENGE FOR THE POLYMER SCIENTIST AND ENGINEER

Joachim Meissner

Institut für Polymere, Eidg. Techn. Hochschule (ETH) Zürich, Switzerland

Abstract - The rheological properties of thermoplastic polymer melts sensitively depend on the chemical and physical structure of the melt, and they reflect the processing behaviour of the polymer investigated. In addition, due to the rheological and thermal pre-history, they are responsible for the anisotropy of the end-use properties of polymeric solids. The conventional methods of polymer melt rheometry cannot provide sufficient information. For a more general investigation, new types of testing were developed: simple elongation and different modes of multiaxial elongation. For these flows, a new classification and new definitions of elongational viscosities were introduced by means of which an efficient comparison with the linear viscoelastic behaviour in shear is easily possible. In more recent tests, both shear and elongational flows were performed with a change of the principal axes of the deformation rate such that the rheological consequences of a deformation-induced anisotropy can be studied. For all cases, examples of test results will be given. Finally, the central role of polymer melt rheology for the different aspects of polymer science and engineering is elucidated.

INTRODUCTION

For thermoplastic polymers the rheological behaviour of the melts is linking the scientific interests of polymer chemists and physicists with the practical interests of polymer engineers. Polymer melt rheology is incorporated in the main subject of polymer science and engineering, i.e. the relationships between polymer structure (in the most general sense) and the end-use properties of final parts made out of plastics (Refs. 1 - 3).

Polymer melt rheology means a challenge for many of us because the rheological properties of the melts (i) are extremely sensitive to the molecular structure, (ii) reflect the processing behaviour of thermoplastics, and (iii) exercise an influence on the physical and technological properties of polymeric solids according to the rheological and thermal pre-history.

Melt rheology means a challenge to rheologists because the central problem is not yet solved, and this is the formulation of a "correct" (and workable) constitutive equation which describes the stress at any instant of flow as a function of the deformation history up to this instant. The lack of the constitutive equation for polymer melts is caused by their complicated and insufficiently investigated rheological behaviour. During the past and also presently, the experimental tools available were and are too limited. As a consequence, conclusions drawn from this limited knowledge lead to wrong predictions about the behaviour under more general flow situations.

In the following, after a short presentation of the melt as a pseudoplastic, viscoelastic, rubberlike liquid, a short review on experimental methods shall be given with special emphasis on new modes of testing and with new results from which follows that only by new experimental means the general behaviour can be investigated and guidelines be established for the further theoretical development. Concerning the present conventional methods reference is made to DEALY (Ref. 4).

RHEOLOGICAL FACTS IN MELT EXTRUSION

Already in melt extrusion, the rheological properties of polymer melts are elucidated. In Fig. 1 the melt is extruded by extrusion pressure p out of a die (I) with output rate q. At a tenfold extrusion pressure the output rate increases by much more than by the factor 10. From this follows that the viscosity decreases with increasing mechanical action: polymer melts are *pseudoplastic liquids*.

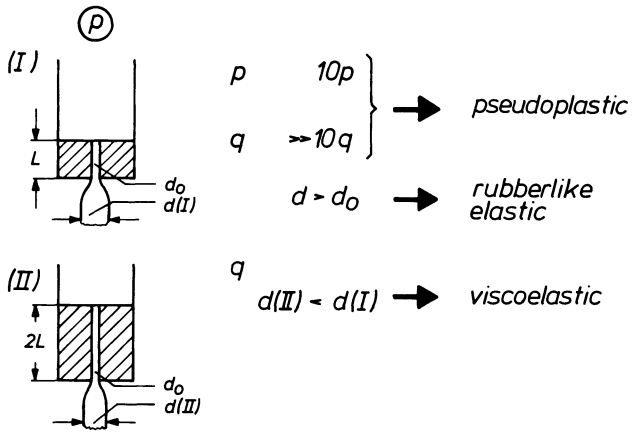

Fig. 1 Demonstration of the rheological properties of polymer melts in melt extrusion through a die of a capillary rheometer.

The diameter of the strand emerging from the die, can have a much larger diameter d than the die diameter d_0. This extrudate swell is caused by the orientation of the molecules in front of and within the die. Outside the die this orientation recovers causing a macroscopic shrinkage of the emerging strand and an increase of the extrudate diameter. Obviously, large, entropy-elastic deformations exist in polymer melt flows, hence, polymer melts are *rubberlike liquids*. The connection between viscous flow and elastic deformation depends on flow time which is illustrated by the extrudate diameters of the two dies (I) and (II) of Fig. 1. As a consequence, polymer melts are *viscoelastic liquids*.

With different, important corrections the output rate - pressure curves obtained from the capillary rheometer can be converted into the viscosity function $\eta(\dot{\gamma})$ where $\dot{\gamma}$ is the shear rate (Ref. 2). For three different polystyrene melts the curves $\eta(\dot{\gamma})$ are given in Fig. 2 which demonstrate the tremendous decrease of the viscosity with increasing shear rate (Ref.5). For polymer processing the range of higher shear rates is important where the three curves coincide.

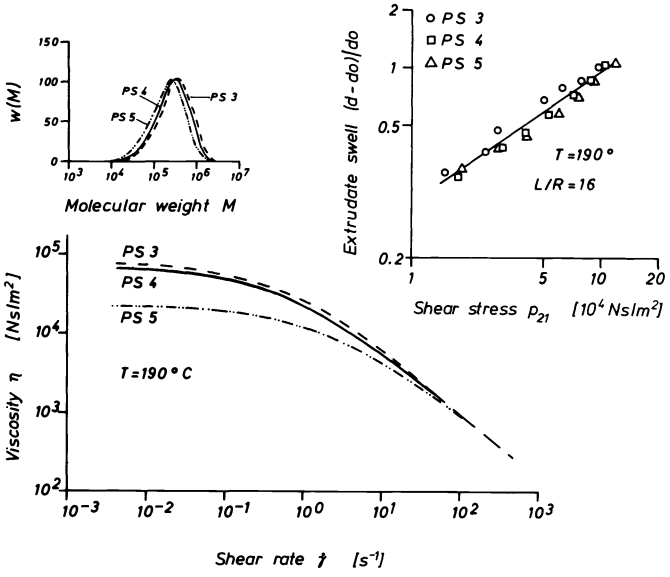

Fig. 2 Viscosity functions and extrudate swell for three polystyrene melts characterized by slightly different molecular weight averages but similar molecular weight distributions. The viscosity at low shear rates was measured in a rotational instrument, for higher shear rates a capillary rheometer was used, compare H. MUENSTEDT (Ref. 5).

At low shear rates, however, the differences are remarkable, especially for the zero shear

viscosity $\eta_0 = \lim \eta(\dot{\gamma})$ with $\dot{\gamma} \to 0$, and the well-known relation $\eta_0 \alpha M_W^{3.5}$ holds. This means that for the polymer chemist who wants to grade and characterize the material by melt rheology, the range of low shear rates is more important because differences between the viscosity functions of different products are more obvious. Fig. 2 also gives results for the extrudate swell which reflects to a certain degree the elastic deformation of the melt connected in capillary flow. There is no difference in extrudate swell of the three polystyrene melts with the data plotted as a function of shear stress.

For melts with equal weight average molecular weight M_W but different molecular weight distributions Fig. 3 shows the opposite rheological consequences: The viscosity functions are similar but the elastic deformations expressed as extrudate swell are different.

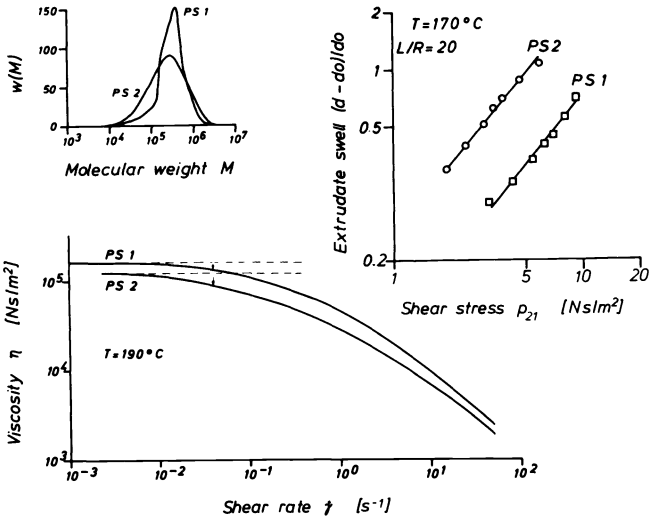

Fig. 3 Viscosity functions and extrudate swell for polystyrene melts characterized by a similar weight average M_W but different molecular weight distributions (Ref. 5).

We can conclude from this short illustration that for different scientific and engineering aspects different parts of the viscosity function are important and that the different molecular parameters have a different influence on the rheological properties of the melts.

THE VISCOSITY FUNCTION

The decrease of the viscosity with increasing mechanical action must be inherent in the long, flexible macromolecules independent of chemical parameters, especially molecular weight, and independent of temperature and hydrostatic pressure: For many polymer melts VINOGRADOV and MALKIN (Ref. 6) were successful in finding within a narrow bandwidth the same function by plotting the reduced coordinates η/η_0 as a function of $\eta_0\dot{\gamma}$, compare Fig. 4, as was reviewed by SEMJONOW (Ref. 7). $\eta_0\dot{\gamma}$ has the meaning of a nominal shear stress.

The existence of a general reduced viscosity function like that of Fig. 4 indicates (i) that the correct reduction parameter is η_0 which incorporates the influence of chemical structure, temperature and hydrostatic pressure on the viscous flow, (ii) that for engineering purposes this reduced viscosity function can be expressed by a simple analytical expression describing the viscous behaviour in a reasonable good approximation given in (Ref. 6), (iii) that even when the laminar flow is terminated by a flow instability called melt fracture (Ref. 8) the concept of the viscosity function seems to be justified because the curves of Fig. 4 are steady (see Note a). The melt fracture phenomenon starts to occur, e.g. for LDPE melts, already at a reduced viscosity of $\eta/\eta_0 = 0.02 - 0.03$ (Ref. 9).

Note a: Some linear polymers (e.g. HDPE) show an instantaneous increase of the output rate in the capillary rheometer as soon as melt fracture occurs (Ref. 9) resulting in a jump-like decrease of the viscosity function.

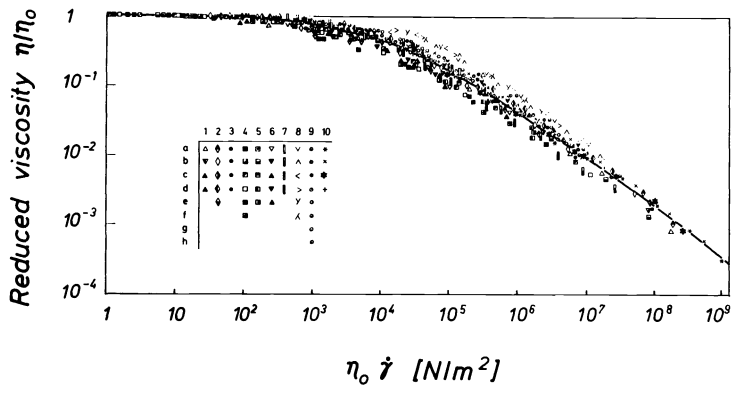

1 LDPE: a = 170, b = 190, c = 210, d = 230°C
2 PP: a = 190, b = 210, c = 230, d = 250, e = 270°C
3 PS: a = 170, b = 190, c = 210, d = 230°C
4 PE (ς = 0.914): a = 108, b = 125, c = 140, d = 174, e = 206, f = 230°C
5 PE (ς = 0.923): a = 112, b = 125, c = 175, d = 190, e = 250°C
6 PE: a = 130, b = 150, c = 170, d = 190, e = 210°C
7 PVB: a = 119, b = 125, c = 139, d = 155°C
8 Natural rubber: a = 50, b = 60, c = 80, d = 100, e = 120, f = 140°C
9 PIB: a = -5, b = 0, c = 10, d = 20, e = 40, f = 60, g = 80, h = 100°C
10 Synthetic rubber: a = 40, b = 60, c = 80, d = 120°C

Fig. 4 Reduced viscosity function after VINOGRADOV et al. reviewed by SEMJONOW (Ref. 7).

LINEAR VISCOELASTICITY

The viscosity function $\eta(\dot{\gamma})$ is not sufficient for a general knowledge of the rheological behaviour of polymer melts, because from $\eta(\dot{\gamma})$ no information is available about the time or frequency dependent material response. Since LEADERMAN's work (Ref. 10) the linear viscoelastic investigation of polymeric solids is well established. The test methods are included in international standards and the theory is well worked out (Ref. 11). For polymer melts, it is very recent that equivalent methods are introduced in industry although a first detailed collaborative investigation was already performed in 1956 with N.B.S. polyisobutylene (a polymer melt at room temperature!) (Ref. 12).

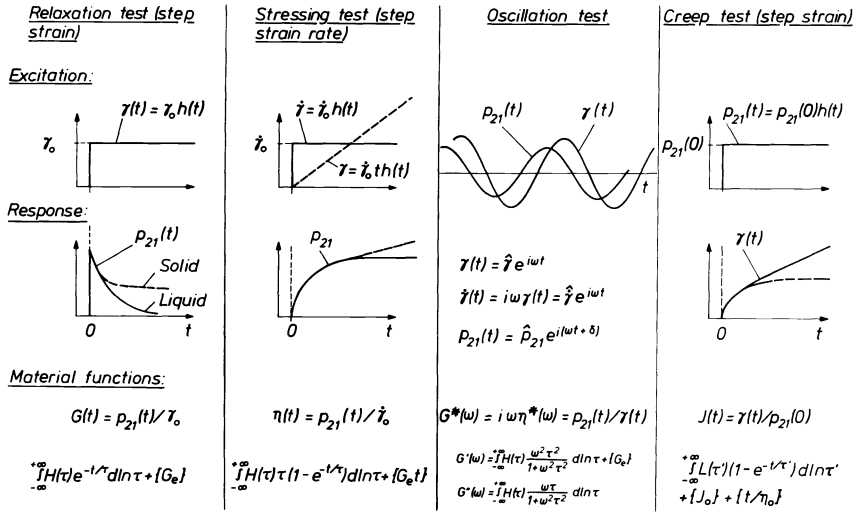

Fig. 5 Basic tests in linear viscoelasticity for solids and liquids, formulated for the deformation in shear.

In Fig. 5 the most important test methods in linear viscoelasticity are summarized. From these tests the spectra of relaxation $H(\tau)$ and retardation $L(\tau')$ follow which represent the distribution functions of the molecular motions in the melt occuring with certain relaxation or retardation times and with certain contributions to the instantaneous modulus. The test with the step function strain rate (*stressing test* according to GIESEKUS (Ref. 13)) is particularly adequate for liquids: The stress growth curve terminates in an equilibrium value from which the zero shear viscosity $\eta_0 = \lim_{\dot{\gamma}\to 0,\ t\to\infty} \eta(t,\dot{\gamma})$ follows.

As an example, creep results in elongation are shown in Fig. 6 for polystyrene samples of different molecular weight distributions but similar M_W (Ref. 14). For the material with the broader distribution the curved range of the creep curve is much longer indicating that already in the linear viscoelastic behaviour the influence of the molecular weight distribution is reflected.

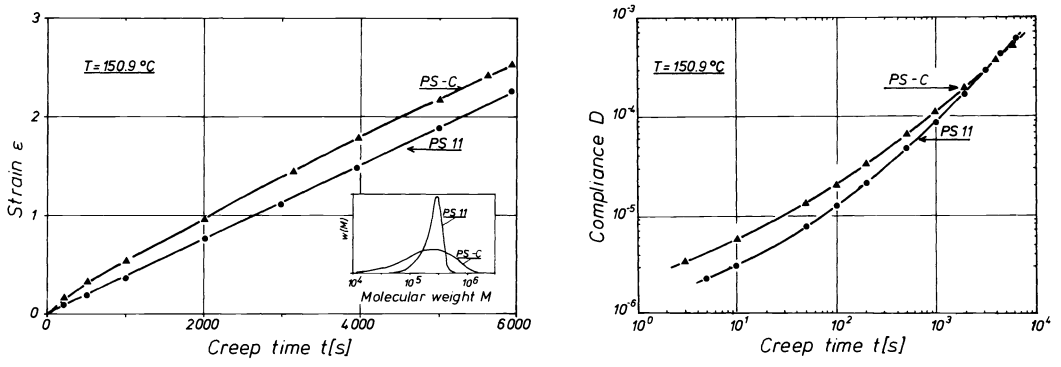

Fig. 6 Creep curve $\varepsilon(t)$ in elongation and elongational creep compliance D(t) of polystyrene samples of different molecular weight distributions (Ref. 14).

From the practical point of view it should be mentioned that studies in the linear range require only a small amount of sample but there are only a few instruments available commercially which are especially designed for the investigation of the linear properties of polymer melts.

SIMPLE SHEAR AND VISCOMETRIC FLOWS

In simple shear flow of polymer melts the deformation rate tensor

$$\underline{\underline{\dot{\varepsilon}}}(t) = \frac{1}{2}(\nabla\underline{v}+\nabla\underline{v}^T) = \frac{1}{2}\dot{\gamma}(t)\begin{pmatrix}0 & 1 & 0\\ 1 & 0 & 0\\ 0 & 0 & 0\end{pmatrix} \tag{1}$$

and the stress tensor

$$\underline{\underline{p}} = \begin{pmatrix}p_{11} & p_{12} & 0\\ p_{21} & p_{22} & 0\\ 0 & 0 & p_{33}\end{pmatrix} \tag{2}$$

do not have the same principal axes because the three normal stress components are different from each other. In these equations $\underline{v}$ is the velocity vector, $\nabla\underline{v}$ the velocity gradient, and $\nabla\underline{v}^T$ its transpose. With the condition of incompressibility

$$\nabla\cdot\underline{v} = 0 \tag{3}$$

only two normal stress differences are rheologically relevant,

$$N_1 = p_{11} - p_{22} \quad \text{and} \quad N_2 = p_{22} - p_{33} \tag{4},$$

in addition to the shear stress $p_{21} = p_{12}$.

With material surfaces instead of material planes sliding along each other the same results follow with the embedded unit vector $\check{e}_1$ in the direction of flow, $\check{e}_2$ for the normal vector of the shear surfaces, and $\check{e}_3 = \check{e}_1 \times \check{e}_2$ representing the third direction. In this case we speak of *viscometric flows* (Ref. 15) if the shear rate $\dot{\gamma}(t)$ follows a step function with the constant shear rate $\dot{\gamma}_0$

$$\dot{\gamma}(t) = \dot{\gamma}_0 h(t) \tag{5}.$$

From the equation of motion for the melt in the gap of a cone-and-plate rotational rheometer it follows that the two normal stress differences can be obtained from the radial pressure distribution by means of the relations given in Fig. 7 (Ref. 16), and that the normal force

which tends to separate the cone and the plate, is connected with N_1. It was WEISSENBERG who described the first instrument for the simultaneous measurement of p_{21} and N_1 (Ref. 17) for liquids of low viscosity. With polymer melts the first measurements of p_{21}, N_1 and N_2 were performed by POLLETT in 1955 (Ref. 18). His results show already the main features of the rheological behaviour of polymer melts in shear flow.

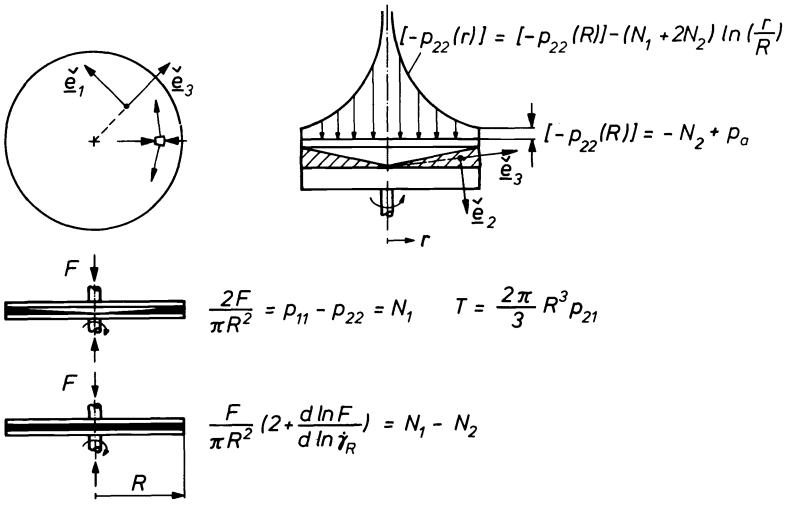

Fig. 7 Relations for the determination of stress components in shear flow of elastic liquids between cone-and-plate.

With a further modification of the cone-and-plate instrument it was possible to measure in addition to p_{21} and N_1 also the elastic recovery γ_R (Ref. 19). For a melt of low density polyethylene (LDPE) the results are given in Fig. 8. It is evident that all three quantities measured have a pronounced maximum, and that the maxima of N_1 and γ_R are remarkably high. This means that at the onset of shear, polymer melts are deformed elastically with very large elastic strain portions until with increasing shear the physical structure of the melt "breaks down", in other words after the rubberlike, very elastic deformation of the melt, γ_R and N_1 decrease with further increase of the total shear strain. The conclusion from this behaviour is that the structure of the physical network of the melt is changed due to shear deformation.

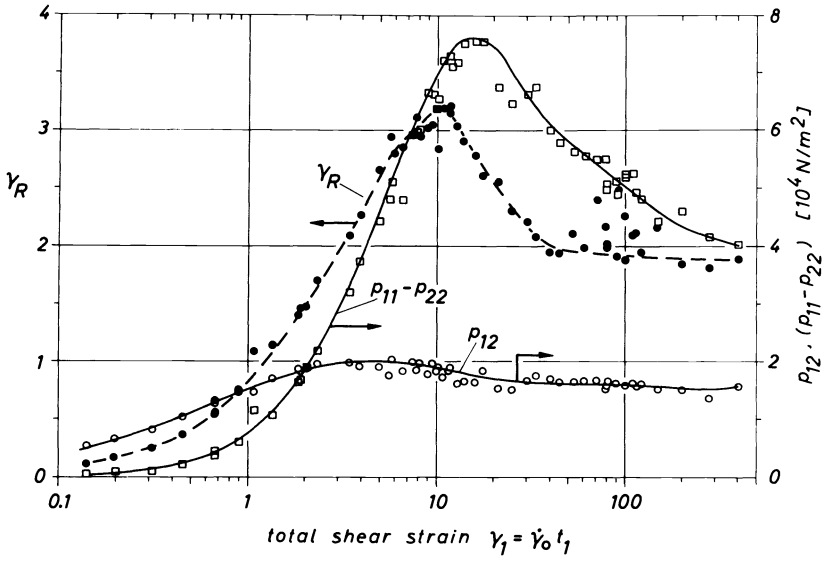

Fig. 8 Shear stress $p_{21} = p_{12}$, first normal stress difference $N_1 = p_{11} - p_{22}$ and total recovery γ_R for a low density polyethylene melt at a shear rate of $\dot{\gamma}_0 = 2\ s^{-1}$ and 150°C (Ref. 19).

The decrease after the maxima and the equilibrium values for N_1 and γ_R cannot be observed accurately enough because disturbances arise at the free surface of the sample starting from the rim. This has been investigated recently by a special experimental set-up: the lower plate is made out of glass and illuminated. With this device shwon in Fig. 9 GLEISSLE could observe the onset and the development of the disturbances, and he made several proposals for the design of screening rings in order to avoid this difficulty (Ref. 20). Another source of error arises because of the elastic properties of the instrument itself (Ref. 21).

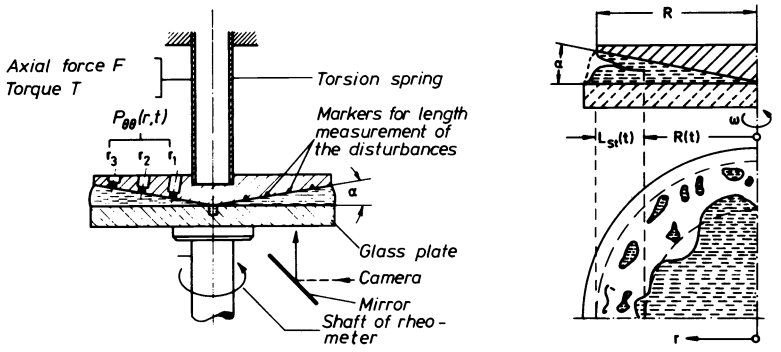

Fig. 9 Experimental device for the investigation of the development of instabilities in cone-and-plate shear flow of polymer melts. W. GLEISSLE 1978 (Ref. 20).

The test results of Fig. 8 illustrate the combined influence of time and deformation during shear flow. This influence could be separated by relaxation tests of different, including large steps of shear strain γ_0. In the cone-and-plate apparatus, not only the torque (p_{21}) but also the normal force (N_1) were recorded. The results obtained by LAUN (Ref. 22) with an instrument as in Fig. 7 are given in Fig. 10. From these results it follows that the influence of time and shear strain on the relaxation modulus can be separated into a product with an attenuation function $h(\gamma_0)$ introduced by WAGNER (Ref. 23):

$$G(t,\gamma_0) = \overset{0}{G}(t)h(\gamma_0) = p_{21}(t)/\gamma_0 = N_1(t)/\gamma_0^2 \qquad (6)$$

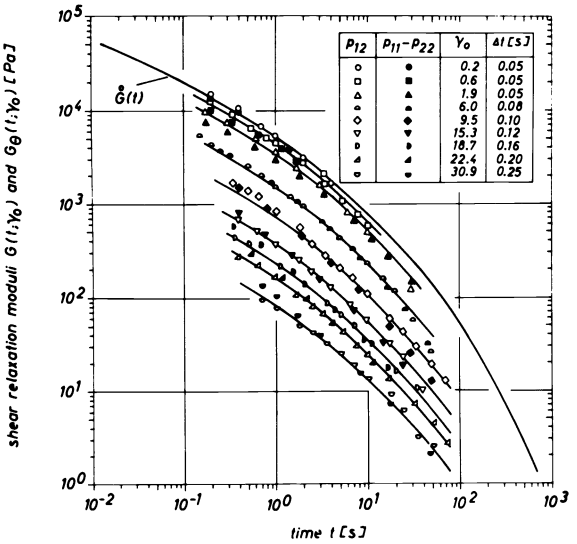

Fig. 10 Shear relaxation modulus from relaxation tests with different step hights γ_0 of the shear deformation. Cone-and-plate rheometer with results from shear stress and first normal stress measurements. H.M. LAUN 1978 (Ref. 22).

GENERAL SHEAR FLOWS

Up to now all our investigations were performed in unidirectional shear flow only. This restriction may provide insufficient information with respect to processing when the direction of flow changes causing a re-orientation of the molecules into the new flow direction. The molecular orientation inherent in shear flow represents a shear induced anisotropy yielding different flow properties in different directions when the direction of flow is altered. Such a situation occurs several times in a processing machine, and the question is whether the consequences of this shear induced anisotropy must be taken into consideration.

In order to clarify this problem experimentally, a new sandwich-type shear rheometer was developed (Ref. 24), which is shown in Fig. 11. The sample S consists of two thin polymer melt films located between a central plate (CP) fixed to the frame of the instrument by force measuring devices (SF, TF), and two outer plates (UP, LP). They are clamped together forming a carriage which can be moved into the directions x_1 and x_3 independently of each other.

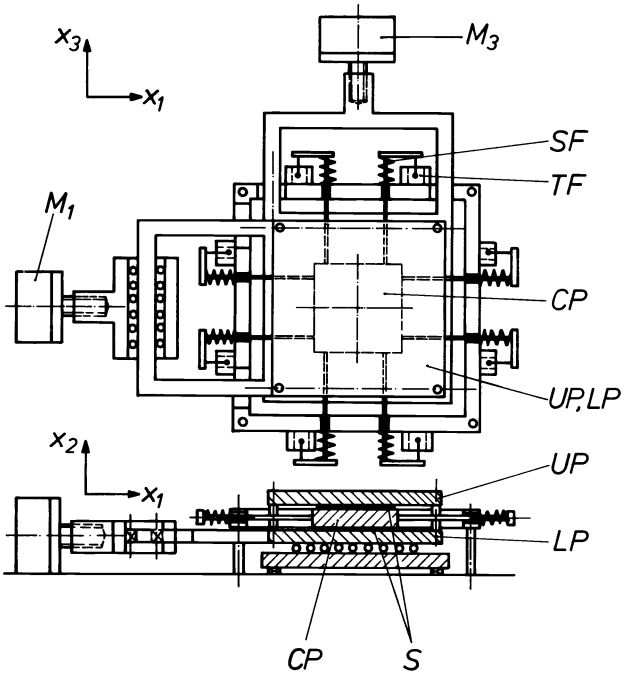

Fig. 11 Schematic diagram of a sandwich-type biaxial shear rheometer for arbitrary shear deformations in two directions x_1 and x_3 (Ref. 24)

For a preliminary test result a polyisobutylene melt (OPPANOL B15) was sheared at a shear rate of $\dot{\gamma}_{21} = \dot{\gamma}_0 = 0.1\ s^{-1}$ in the direction x_1 up to a certain instant t_c at which the shear direction was changed by starting the additional movement in the direction x_3 with $\dot{\gamma}_{23} = \dot{\gamma}_0$. The resulting stress components are shown in Fig. 12.

From these results the following preliminary conclusions can be drawn: (i) Up to t_c the shear stress p_{21} reflects the normal behaviour already discussed in connection with Fig. 8. (ii) With the start of the additional $\dot{\gamma}_{23}$ at t_c, the new stress component p_{23} shows a growth which seems to be independent of t_c and similar to that of p_{21} at the start of the test at $t = 0$, (iii) during the first few seconds after t_c, the curves of p_{21} do not show any change due to the onset of $\dot{\gamma}_{23}$, (iv) finally, p_{21} decreases and p_{23} increases further until both components are equal. This requires approximately 30 s after t_c. During this period of time, the influence of the pre-orientation of the molecules due to the initial flow prior to t_c is noticed as anisotropy: The two shear stress components belonging to the same shear rate are different for a remarkably long period of time.

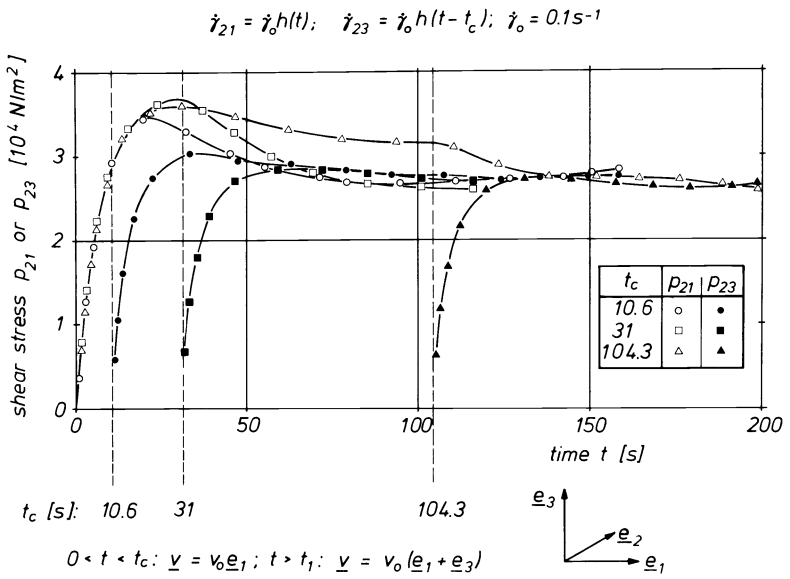

Fig. 12 Shear stresses p_{21} and p_{23} at the change of the directions of shear flow with the following shear history: $\dot\gamma_{21} = \dot\gamma_0 h(t)$; $\dot\gamma_{23} = \dot\gamma_0 h(t - t_1)$, $\dot\gamma_0 = 0.1\ s^{-1}$. Polyisobutylene ("OPPANOL B15") at 23°C (Ref. 24).

ELONGATIONAL FLOWS WITH CONSTANT STRAIN RATES

During the last ten years, a remarkable progress could be achieved in elongational rheometry (Ref. 25). We do not give experimental details here but present Fig. 13 with the shear and elongational viscosities obtained in simple shear and simple elongation, respectively, for the same polymer melt (Refs. 21&26). At still higher total strains, well-developed maxima of the elongational viscosities were found (Ref. 27). The data of Fig. 13 demonstrate the opposite behaviour of the melt in shear and elongation, i.e. shear thinning and elongational hardening. It should be mentioned, however, that the rubberlike liquid theory of LODGE, where the strain measure is the relative FINGER tensor, predicts still higher stresses in elongation (Ref. 28) such that from the point of view of this theory the melt is thinning both in elongation and in shear (Ref. 29).

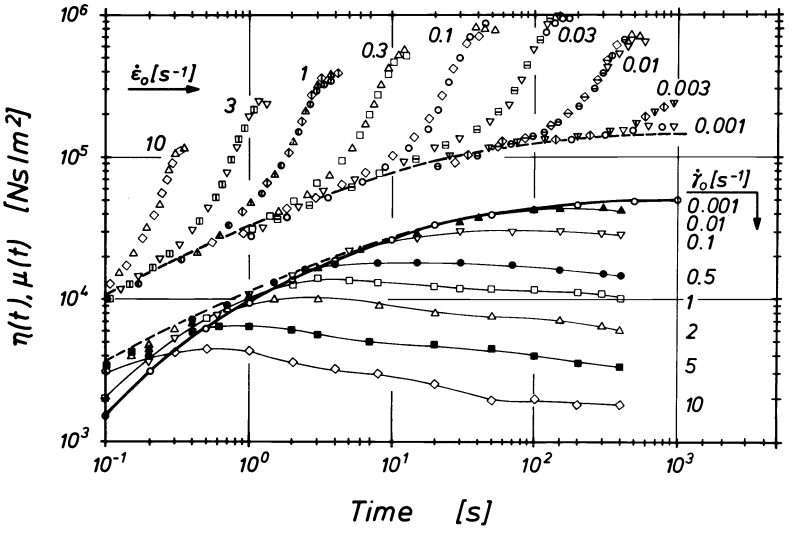

Fig. 13 Shear and elongational viscosities of a low density polyethylene melt at a temperatur of 150°C, after LAUN (Ref. 26) and MEISSNER (Ref. 21).

For the treatment of engineering problems with elongational flows it is an important conclusion from Fig. 13 that there is, in general, no rheologically steady state in simple elongation with a constant viscosity and that the elongational viscosity at a higher strain rate is much larger than the shear viscosity. Therefore, elongational flows like in melt spinning cannot be treated by the threefold of the shear viscosity measured at a corresponding shear rate.

The contrast of the melt behaviour in simple shear and simple elongation raises the question about the behaviour at other flow modes like equibiaxial elongation important in processes like film and bottle blowing. Also from a more general point of view, polymer melts should be investigated in different elongational flows in order to obtain more general answers.

For the case of elongational flows with constant strain rates a new classification was given and it was demonstrated that these flows can be realized with polymer melts (Refs. 30&31). With the incompressibility condition and the principal strain rates ordered according to Fig. 14, the strain rate tensor follows with the maximum strain rate $\dot{\varepsilon}_0 = \dot{\varepsilon}_{11}$ and the test mode $m = \dot{\varepsilon}_{22}/\dot{\varepsilon}_{11}$. Each test is indicated by a point in the hatched area of the $\dot{\varepsilon}_{11}$ - $\dot{\varepsilon}_{22}$-plane, Fig. 14. There are three special cases: m = - 1/2 (simple elongation), m = 1 (equibiaxial elongation) and m = 0 (planar elongation).

$$\underline{\underline{\dot{\varepsilon}}} = \frac{1}{2}\left\{ \nabla\underline{v} + (\nabla\underline{v})^T \right\}$$

incompressible: $\nabla\cdot\underline{v} = \dot{\varepsilon}_{11} + \dot{\varepsilon}_{22} + \dot{\varepsilon}_{33} = 0$

general elongation: $\dot{\varepsilon}_{ij} = 0 \quad (i \neq j)$

constant $\dot{\varepsilon}$: $\dot{\varepsilon}_{11} \equiv \dot{\varepsilon}_0 \geq \dot{\varepsilon}_{22} \geq \dot{\varepsilon}_{33}$

test parameter: $m \equiv \dot{\varepsilon}_{22}/\dot{\varepsilon}_{11} = \dot{\varepsilon}_{22}/\dot{\varepsilon}_0$

$$\underline{\underline{\dot{\varepsilon}}}(t) = \dot{\varepsilon}_0\, h(t) \begin{pmatrix} 1 & 0 & 0 \\ 0 & m & 0 \\ 0 & 0 & -(1+m) \end{pmatrix}$$

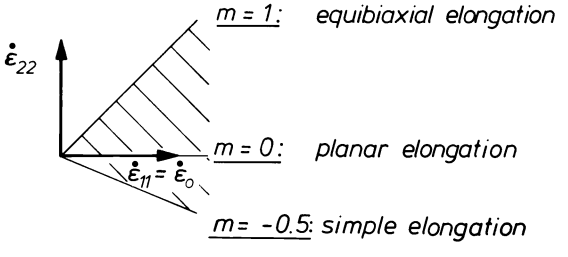

Fig. 14 Classification and representation of multiaxial elongational flows with constant strain rates (Refs. 30&31).

The experimental key to the realization of these multiaxial flows is the rotary clamp the development of which was already described in detail (Ref. 32). A modified clamp (Ref. 31) is shown in Fig. 15. This clamp consists of two grooved cylinders RC with a stepping motor inside. A sheetlike sample of polymer melt is pulled through the nip line between the cylinders and wound-up by the third cylinder WU. The clamp is mounted on a base plate BP connected with a frame plate FP and a suspension plate SP. The connections are made by leaf springs in such a way that their displacements correspond to the force components in the length and perpendicular directions of the clamp. By means of two transducers (TL and TN) these two force components acting on the sample at the nip line of the cylinders RC can be recorded simultaneously.

For equibiaxial elongation, eight such rotary clamps are arranged in a circle and all the clamps rotate with the same constant speed. The elongation follows from a grid which is photographed, and it turns out that the elongation is remarkably homogeneous (Refs. 30&32). The sample is polyisobutylene with the shape of a circular disc of approximately 330 mm diameter and an initial thickness of 5 mm. For planar elongation, the clamps are arranged in a rectangle as shown in Fig. 16 (Refs. 31&33). The scissors cut the sample intermittently at the rim into bands which are wound-up on top of the clamps. Furthermore, the scissors reproducibly provide the reference area formed by width W_c and length L_c. It follows from Fig. 16 that two independent stress components are obtained: (i) the stress $\sigma_1 = p_{11} - p_{33}$ connected with the elongation in the direction x_1 and (ii) the stress $\sigma_2 = p_{22} - p_{33}$ which prevents the lateral contraction in the direction x_2.

For a definition of material functions representing the behaviour in multiaxial elongational flows the constitutive equation should be known. However, we only know that for small excitations polymer melts behave linear viscoelastic. The constitutive equation of linear viscoelasticity is given in Fig. 17 together with the stress tensors for simple shear and multiaxial elongational flows. From this equation, the normal stress differences σ_i for elongation follow with the same integral of the relaxation modulus as for the shear stress in simple shear flow. This integral defines the transient linear viscoelastic shear viscosity (= stressing viscosity) $\overset{0}{\eta}(t)$.

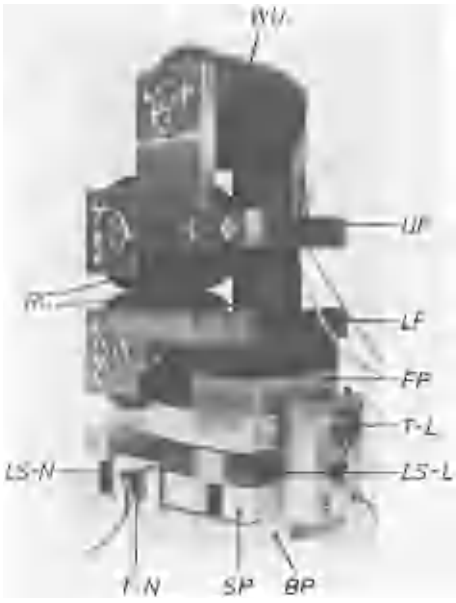

Fig. 15 Rotary clamp for multiaxial elongation of polyisobutylene. The symbols are explained in text, for more experimental details see Ref. 31.

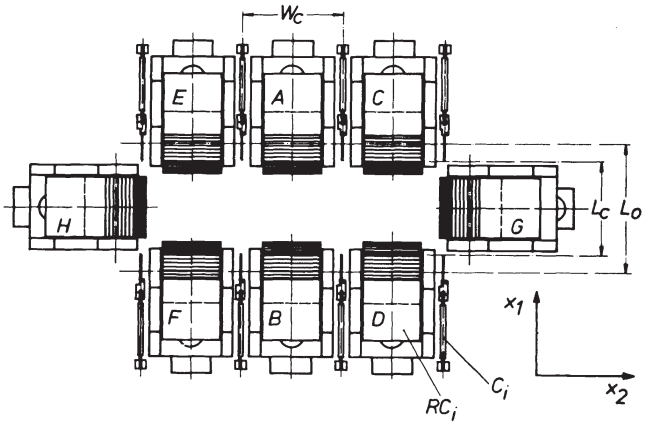

Fig. 16 Rectangular arrangement of eight rotary clamps for the performance of planar elongational flows. The clamps H and G do not rotate but keep the sample clamped in the x_2-direction. Eight scissors C_i cut the sample intermittently. Thus, the reference area formed by length L_c and width W_c is well defined.

$$\boxed{\underline{\underline{p}}(t) + p\,\underline{\underline{1}} = 2\int_{-\infty}^{t} \overset{\circ}{G}(t-t')\,\underline{\underline{\dot{\varepsilon}}}(t')\,dt'}$$

simple shear: $$\underline{\underline{\dot{\varepsilon}}}(t) = \frac{1}{2}\dot{\gamma}_o h(t)\begin{pmatrix}0&1&0\\1&0&0\\0&0&0\end{pmatrix}; \quad \underline{\underline{p}} = \begin{pmatrix}0&p_{12}&0\\p_{21}&0&0\\0&0&0\end{pmatrix}$$

$$p_{21}(t) = \dot{\gamma}_o \int_o^t \overset{\circ}{G}(t-t')dt' = \dot{\gamma}_o \overset{\circ}{\eta}(t)$$

elongation: ($\dot{\varepsilon}_{ii}$ = const.) $$\underline{\underline{\dot{\varepsilon}}}(t') = \dot{\varepsilon}_o h(t')\begin{pmatrix}1&0&0\\0&m&0\\0&0&-(1+m)\end{pmatrix}; \quad \underline{\underline{p}} = \begin{pmatrix}p_{11}&0&0\\0&p_{22}&0\\0&0&p_{33}\end{pmatrix}$$

$$\sigma_1 \equiv p_{11} - p_{33}; \quad \sigma_2 = p_{22} - p_{33}; \quad \sigma_{33} = p_{11} - p_{22}\,(= \sigma_1 - \sigma_2)$$

$$\sigma_1(t) = 2(2+m)\,\dot{\varepsilon}_o \int_o^t G(t-t')dt' = 2(2+m)\dot{\varepsilon}_o \overset{\circ}{\eta}(t)$$

$$\overset{\circ}{\mu}_1(t) = A_1\sigma_1(t)/\dot{\varepsilon}_o = \overset{\circ}{\eta}(t) = \int_o^t G(t-t')\,dt'; \quad A_1 = \frac{1}{2(2+m)}$$

$$\overset{\circ}{\mu}_2(t) = A_2\sigma_2(t)/\dot{\varepsilon}_o = \overset{\circ}{\eta}(t) = \int_o^t G(t-t')\,dt'; \quad A_2 = \frac{1}{2(1+2m)}; \quad (m \neq -0.5)$$

$$\overset{\circ}{\mu}_3(t) = A_3\sigma_3(t)/\dot{\varepsilon}_o = \overset{\circ}{\eta}(t) = \int_o^t G(t-t')\,dt'; \quad A_3 = \frac{1}{2(1-m)}; \quad (m \neq 1)$$

Fig. 17 Linear viscoelastic constitutive equation and definition of transient elongational viscosities $\mu_i(t)$ in multiaxial elongation with constant strain rates.

In the expressions for the normal stress differences σ_i we denote this integral by μ_i and take the influence of the test mode m into the front factors A_i (Refs. 30&31). With these definitions, the elongational viscosities and the shear viscosity are equal for the linear case. We keep the definitions also for the nonlinear case with the advantage that the nonlinear behaviour under different test modes m in elongation can be compared with the linear behaviour represented by $\overset{o}{\eta}(t)$.

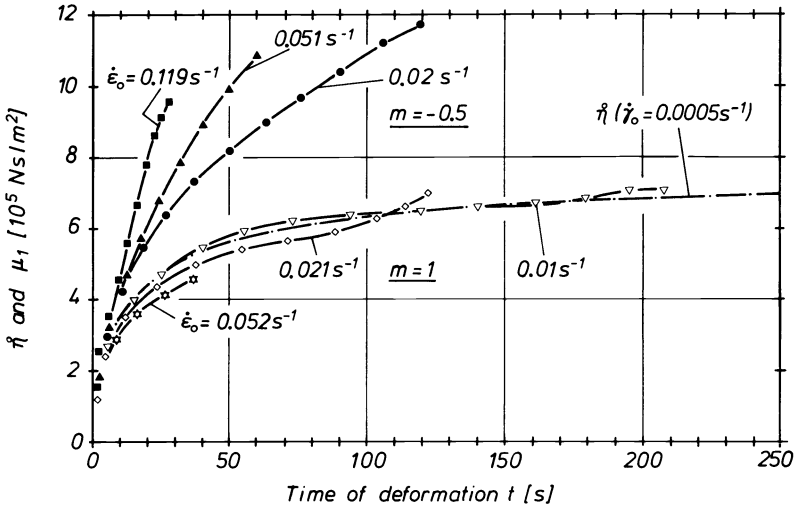

Fig. 18 First elongational viscosity $\mu_1(t)$ for simple elongation (m = - 0.5, filled symbols) and equibiaxial elongation (m = 1, open symbols) for polyisobutylene ("OPPANOL B15") at 23°C (Refs. 31&33). The linear viscoelastic shear viscosity $\overset{o}{\eta}(t)$(-·-·-·-) was kindly measured for us by Dr. H.M. LAUN, BASF Ludwigshafen (Ref. 34).

In Fig. 18 the elongational viscosities are given for simple and planar elongations together with the linear shear viscosity $\overset{o}{\eta}(t)$. Like in Fig. 13 for polyethylene, there is a pronounced strain hardening in simple elongation for the polyisobutylene investigated. The increase of $\mu_1(t) = \mu_3(t)$ above $\overset{o}{\eta}(t)$ is steeper with higher strain rate $\dot{\varepsilon}_0$. For equibiaxial flows the results are opposite: With increasing $\dot{\varepsilon}_0$ the elongational viscosities $\mu_1(t) = \mu_2(t)$ are more below $\overset{o}{\eta}(t)$, however only slightly, and at larger strains there is an inflection and even a crossing with the curve $\overset{o}{\eta}(t)$, as is shown for the two lowest strain rates.

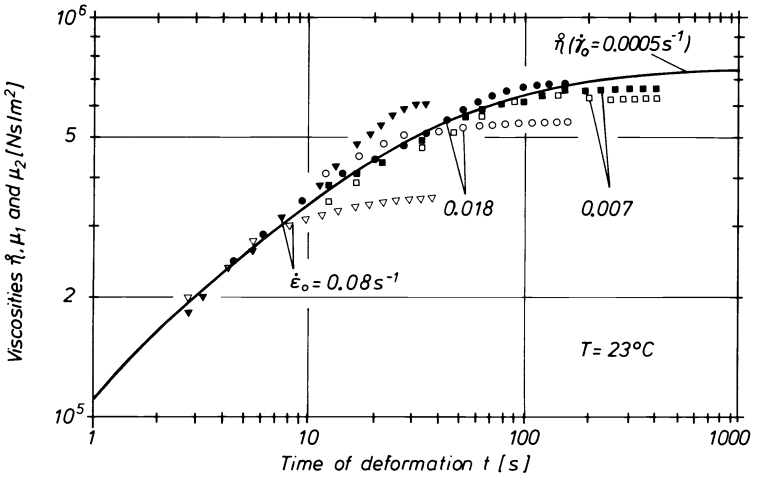

(Test No) μ_1 / μ_2	(121) ■ □	(117) ● ○	(135) ▼ ▽
$\bar{\dot{\varepsilon}}_0$ [s⁻¹]	0.0072	0.0185	0.0815

Fig. 19 Elongational viscosities $\mu_1(t)$ and $\mu_2(t)$ for planar flow (m = 0) of polyisobutylene and comparison with $\overset{o}{\eta}(t)$. Material and test temperature as in Fig. 18.

As was already mentioned, in planar elongation two independent physical answers are obtained, i.e. μ_1 and μ_2 which are equal only in the linear range of deformation. In fact, they coincide with $\overset{0}{\eta}(t)$ for the lowest strain rate during the total time of deformation and for the two other strain rates during the onset of the deformation, as is shown in Fig. 19. For larger deformations, however, these two elongational viscosities show an opposite behaviour: Hardening of $\mu_1(t)$, i.e. an increase above $\overset{0}{\eta}(t)$, but thinning of $\mu_2(t)$, i.e. lower values than $\overset{0}{\eta}(t)$.

It should be mentioned that these planar tests are the first ones performed with a polymer melt at constant strain rates and both elongational viscosities measured simultaneously (Refs. 31&33). The contribution of these results to the question of the constitutive equation was already discussed in Ref. 31. The versatility of the new rheometer also allows new tests to be performed, e.g. with m = + 1/2 (Ref. 33).

STRAIN INDUCED ANISOTROPY IN ELONGATION

With the elongational tests described above there is still the restriction that the strain rates are constant throughout the deformation period such that the direction of the molecular orientation due to deformation remains constant. For more general information, necessary also for the solution of practical problems, the test mode m should be a function of time, in other words the principal axes of the strain rate tensor should be changed during elongational flow similar to the general shear flows described above. With rotary clamps such tests can be performed. It is only necessary to mount each clamp on an additional pivot for the turn of the clamp through a certain angle around the center of the nip line of the two grooved cylinders of Fig. 15.

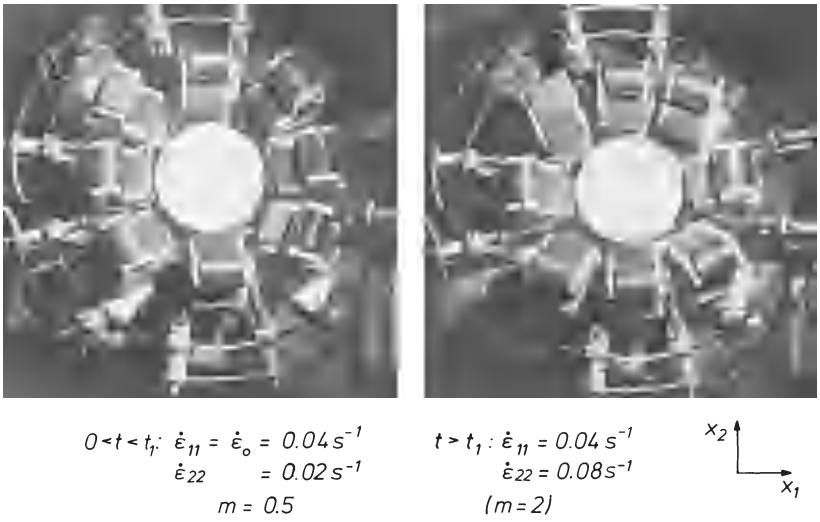

Fig. 20 Multiaxial elongational rheometer for the change of the strain mode m = m(t). Four rotary clamps are mounted on a pivot which can turn the direction of the clamp around the center of the nip line of the two grooved cylinders (RC of Fig. 15). Left: Position of the clamps for a test with m = 0.5. Right: Position after turning the clamps for m = 2. At the time t* of turning, the rotary speed is altered such that the test program indicated in the figure is achieved (Ref. 33).

In Fig. 20 the rheometer is seen from the top, on the left-hand side for a multiaxial elongation with m = + 1/2 and $\dot{\varepsilon}_{11} = \dot{\varepsilon}_o = 0.04\ s^{-1}$. This strain rate $\dot{\varepsilon}_{11}$ has been kept constant during the whole test. At $t^* = \varepsilon_{11}^*/\dot{\varepsilon}_o$ the angular positions of the clamps at the four corners were turned until the positions were attained shown in the picture of the right-hand side of Fig. 20. At the same instant t* the strain rate $\dot{\varepsilon}_{22}$ was increased from 0.02 to 0.08 s-1. Hence, the test mode was changed at t* from m = 0.5 to m = 2. The change of the angular positions of the clamps required two seconds. More experimental details are given in Ref. 33. The measured stresses σ_1 and σ_2 are shown in Fig. 21.

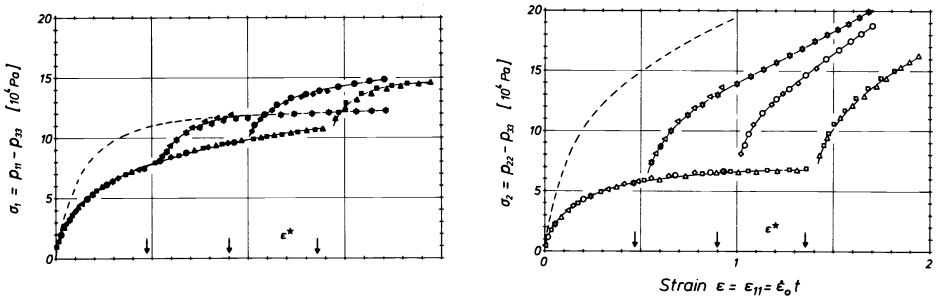

Fig. 21 Stress differences σ_1 and σ_2 in multiaxial elongation with changing m = 0.5 to m = 2 at ε^*. The strain rate $\dot{\varepsilon}_{11} = \dot{\varepsilon}_0 = 0.04\ s^{-1}$ was kept constant throughout the test. Material and temperature like in Fig. 18, (Ref. 33).

Up to the change of m at t* all the curves for σ_1 or σ_2 are equal. After the turn of the clamps at t* the stresses increase remarkably because of the increased $\dot{\varepsilon}_{22} = 2\dot{\varepsilon}_{11} = 2\dot{\varepsilon}_0$ and the change from m = 1/2 to m = 2. The increase of σ_1 seems to attain a steady value for each curve. The increase of σ_2 is very large and this stress grows into a linear increase until the deformation becomes inhomogeneous. For comparison, the results of a test with constant strain rate $\dot{\varepsilon}_0 = 0.08\ s^{-1}$ and m = 1/2 is replotted such that $t^* \to 0$ (curves --- in Fig. 21). The results indicate that the growth of σ_1 and σ_2 is nearly independent of t* or ε^*. The additional stresses due to the change of m and increase in $\dot{\varepsilon}_{22}$ seem to be superposed to the stresses already existing in the material.

CONCLUSIONS AND RELEVANCE TO POLYMER SCIENCE AND ENGINEERING

The given examples of results from different types of rheological investigations reflect the complex behaviour of the melts and lead to the conclusion that only by a systematic experimental planning the general picture of the melt behaviour can be found. Certainly, the different modes of crucial experiments and their minimum number for the determination of the relevant material functions can be derived only from the "correct" constitutive equation which is not yet formulated. It could be shown that in different modes of deformation the main features of the rheological behaviour is determined by different parts of the constitutive equations (Ref. 31). For multiaxial elongation of the polyisobutylene sample referred to in this paper, a comparison of the experimental results with predicitions from different types of network theories is given in Ref. 33.

As was already shown in the beginning of this paper the rheological properties depend sensitively on the molecular structure, and the different parameters of this structure effect the different aspects of the rheological behaviour in a different way, e.g. the molecular weight has a sensitive influence on the zero shear and elongational viscosities, and the molecular weight distribution has so for the elastic recovery of the extrudate swell.

In order to establish precise correlations between the rheological behaviour and the structure of the polymers, the new test methods presented in this paper need further development for (i) higher precision, (ii) higher temperature, and (iii) smaller dimensions. The last point is important in order to work with small samples which are chemically well-defined and specially made for the investigation of structure - properties relationships.

Concerning the engineering aspects, the decrease of the viscosity with increasing shear rate or shear stress, as shown in Fig. 4, is one of the reasons that polymer melts even with high molecular weight can be processed so quickly in extrusion or injection moulding. However, there is until now not much effort to make use of the molecular orientation during flow. ROETHEMEYER demonstrated already in 1969 how to alter the flow history in front of a square-shaped die for the extrusion of square-shaped strands of polyethylene and polyvinylchloride (Ref. 35). Another important contribution is the application of the molecular orientation connected in shear and elongational flows for the remarkable improvement of the end-use properties of polymers: biaxial stretching of standard polystyrene (Ref. 36) and core rotation in injection moulding (Ref. 37). Of course, molecular orientation reflects the stress tensor in melt flow and has been studied also optically by flow birefringence (Ref. 38).

We summarize the interaction of the different aspects of polymer engineering and science by Fig. 22. Polymer melt rheology is required for the development of fluid dynamics and furthermore for a general theory of polymer processing. It reflects and depends sensitively on the structure of the polymer melt, i.e. the chemical structure of the ensemble of single mole-

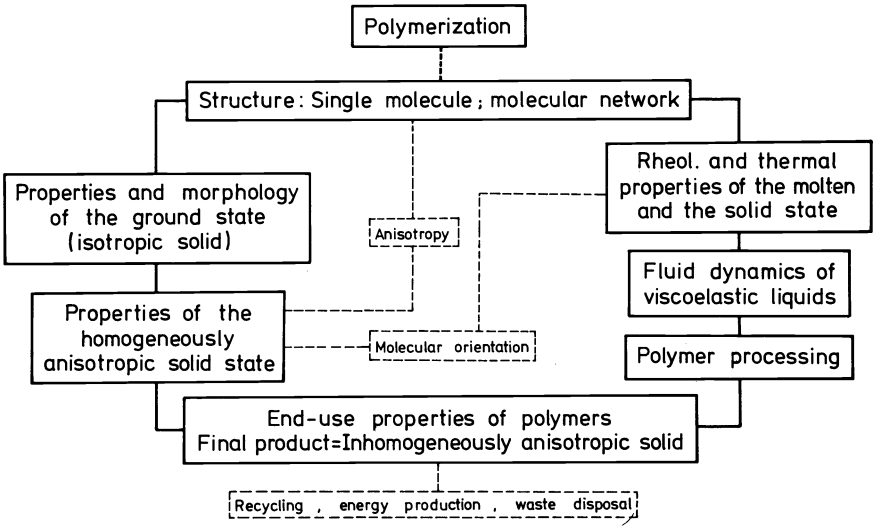

Fig. 22 Problem areas and its interconnections in science and engineering of thermoplastic polymers.

cules and the physical structure of the condensed phase formed by the molecules in the molten state. Rheological properties are responsible for molecular orientations which are frozen-in during the processing due to the rheological and thermal pre-history and which result in an inhomogeneous anisotropy of the technological and physical properties of the final parts produced by processing. Fig. 22 demonstrates the central rôle of polymer melt rheology and reflects its challenge to scientists and engineers fascinated by the field of polymers.

REFERENCES

1. J. Meissner, Chem. Rundschau 28/Nr. 39, 25 (1975)
2. J. Meissner, Pure and Appl. Chem. 42, 553 (1975)
3. H.H. Winter, Pure and Appl. Chem. 55, 943 (1983)
4. J.M. Dealy: Rheometers for Molten Plastics. Van Nostrand Reinhold Comp., New York 1982
5. H. Münstedt in: Praktische Rheologie der Kunststoffe, VDI-Verlag, Düsseldorf 1978
6. G.V. Vinogradov and A.Ya. Malkin, J. Polymer Sci. A2, 2357 (1964)
7. V. Semjonow, Adv. Polymer Sci. 5, 387 (1968)
8. J.P. Tordella, J. Appl. Polymer Sci. 7, 215 (1963)
9. J. Meissner, Kunststoffe 61, 576 and 688 (1971)
10. H. Leaderman: Elastic and Creep Properties of Filamentous Materials and other High Polymers. The Textile Foundation, Washington D.C. 1943
11. J.D. Ferry: Viscoelastic Properties of Polymers, 3rd edition, J. Wiley, New York 1980
12. A.V. Tobolsky and E. Catsiff, J. Polymer Sci. 19, 111 (1956)
13. H. Giesekus, Proc. Fourth Internat. Congr. Rheol. 1963, Part 3, 15. Interscience 1965
14. A. Franck, Ph.D. Dissertation No 7158 ETH Zurich 1982, A. Franck and J. Meissner, Rheol. Acta, to be published
15. B.D. Coleman, H. Markovitz and H. Noll: Viscometric Flows of Non-NEWTONian Fluids. Springer-Verlag, Berlin 1966
16. R.B. Bird, R.C. Armstrong and O. Hassager: Dynamics of Polymeric Liquids: Vol I., J. Wiley, New York 1977
17. S.M. Freeman and K. Weissenberg, Nature 161, 324 (1948)
18. W.F.O. POLLETT, Brit. J. Appl. Phys. 6, 199 (1955)
19. J. Meissner, Rheol. Acta 14, 201 (1975)
20. W. Gleissle, Ph.D. Dissertation, University of Karlsruhe 1978
21. J. Meissner, J. Appl. Polymer Sci. 16, 2877 (1972)
22. H.M. Laun, Rheol. Acta 17, 1 (1978)
23. M.H. Wagner, Rheol. Acta 15, 136 (1976)
24. H.P. Hürlimann and J. Meissner, in preparation
25. C.J.S. Petrie: Elongational Flows, Pitman, London 1979
26. H. Münstedt and H.M. Laun, Rheol. Acta 18, 492 (1979)
27. T. Raible, A. Demarmels and J. Meissner, Polymer Bull. 1, 397 (1979)

28. H. Chang and A.S. Lodge, Rheol. Acta 11, 127 (1972)
29. M.H. Wagner and J. Meissner, Makromol. Chem. 181, 1533 (1980)
30. S.E. Stephenson, Ph.D. Dissertation No 6664, ETH Zurich 1980
31. J. Meissner, S.E. Stephenson, A. Demarmels and P. Portmann, J. Non-NEWTONian Fl. Mechs. 11, 221 (1982)
32. J. Meissner, T. Raible and S.E. Stephenson, J. Rheol.25, 1 (1981)
33. A. Demarmels, Ph.D. Dissertation No 7345, ETH Zurich 1983
34. H.M. Laun, personal communication
35. F. Roethemeyer, Kunststoffe 59, 333 (1969)
36. L.S. Thomas and K.J. Cleereman, SPE-J. 28 (April 1972), p. 61
37. K.J. Cleereman, SPE-J. 25, (Jan. 1969), p. 55
38. H. Janeschitz-Kriegl: Polymer Melt Rheology and Flow Birefringence, Springer-Verlag, Berlin 1983